

# Functionalization of iron oxide nanoparticles with a versatile epoxy amine linker

Michael Nickels,<sup>a</sup> Jingping Xie,<sup>a</sup> Jared Cobb,<sup>ab</sup> John C. Gore<sup>ab</sup> and Wellington Pham<sup>\*ab</sup>

Received 23rd March 2010, Accepted 26th April 2010

First published as an Advance Article on the web 6th May 2010

DOI: 10.1039/c0jm00808g

A synthetically diverse linker molecule consisting of both a terminal epoxide and a terminal amine has been synthesized and shown to have the desired reactivity. Proof of principle experimentation showed that the prepared linker molecule possessed the ability to be reactive towards dextran coated iron nanoparticles, essentially converting the surface alcohols to amines with an efficiency on average of 50 linkers per nanoparticle. Once the surface of the nanoparticles had been functionalized, the iron nanoparticles were subsequently functionalized with both folic acid and fluorescein isothiocyanate, with an average efficiency of 20 and 3 molecules per nanoparticle, respectively. The labeled nanoparticles were then incubated with both folate receptor positive and negative cell lines, which showed a preferential accumulation of the particles in the receptor positive cell line. In addition to the fluorescence based assays, accumulation of the nanoparticles was demonstrated using T2-weighted MRI imaging, which showed that the iron core of the nanoparticle was present within the desired cell line. Overall, this linker has shown the ability to functionalize the surface of nanoparticles and can theoretically be used to label a wide variety of other targeting agents or imaging agents for *in vivo* therapies or diagnostics.

The integration of nanotechnology with molecular imaging in the past decade has made a remarkable impact on biomedical research. In particular, the development of the iron oxide nanoparticles exemplifies this noteworthy advancement. Given their non-toxic, biocompatible, biodegradable characteristics, and their size-dependent design for *in vivo* studies, they have been employed widely in drug delivery,<sup>1,2</sup> bio-sensing,<sup>3</sup> and other biomedical applications such as bio-separation<sup>4,5</sup> and magnetic resonance imaging (MRI) contrast enhancement.<sup>6–9</sup> All of these scientific achievements have relied on the nanoparticles' multivalency, which helps to distinguish iron nanoparticles from other targeting agents. In fact, one functionalized particle can carry multiple copies of an identical biological targeting agent or a mixture of different targeting/imaging agents.

At present, the amine group appears to be an ideal chemical moiety for the functionalization of iron nanoparticles, this is due to its strong nucleophilicity and compatibility with a wide range of available amine activated biological materials. On the other hand, the functionalization of nanoparticles with carboxylic acid groups enables the

conjugation of native peptides, proteins, or antibodies. A number of techniques have been developed for the functionalization of iron oxide nanoparticles, including the *in situ* conversion of dextran hydroxyl groups into amines, which is typically used for the encapsulation of iron core.<sup>10</sup> In the recent work, Young *et al.* coated iron nanoparticles with amine groups using a tripartite component consisting of dopamine, polyethylene glycol (PEG), and trichloro-*s*-triazine.<sup>11</sup> Another approach to fabricating the surface of iron nanoparticles with amine groups uses glycol chitosan.<sup>12</sup> Additional examples include the coating of the iron core with  $\alpha,\omega$ -dicarboxyl-terminated PEG or poly(acrylic acid) to afford the free surface carbonyl groups necessary for further covalent bonding with the targeted molecules.<sup>13,14</sup> Despite all of these achievements, the development of functionalized nanoparticles for targeting imaging still remains a significant problem. Preparation of such probes requires synthetic steps, which make it difficult to analyze the final products.

This paper reports the synthesis and properties of a versatile linker for the surface modification of nanoparticles. The underlying principle of this work is to generate a ready-to-use and water-soluble linker equipped with a highly reactive functional group such as an epoxide. The approach uses dextran-coated nanoparticles developed in our laboratory as a template for such modifications.<sup>15</sup> Since hydroxyl groups on dextran are weak nucleophiles, the use of an epoxide guarantees a neat reaction without the use of a catalyst to enhance the simple reaction work-up. To our knowledge, this is the first report to describe the synthesis of an amine epoxide linker to generate aminated iron oxide nanoparticles.

## Experimental methods

Bovine serum albumin (BSA), folic acid, dicyclohexylcarbodiimide (DCC), fluorescein isothiocyanate (FITC), Fluorescamine, and reaction solvents were obtained from Sigma Chemical Company (St Louis, MO) and used without further purification. Human 293 and A549 cells were obtained from the laboratories of Dr Vito Quaranta and Dr Dennis Hallahan, respectively, at Vanderbilt University. RPMI-1640 medium without folic acid was obtained from Invitrogen.

## Developing superparamagnetic iron oxide (SPIO) nanoparticles

Dextran-coated iron oxide nanoparticles were fabricated in our laboratory using the reported protocol, but with some modifications.<sup>15</sup> In brief, a saturated mixture of dextran and ferric chloride was coalesced with a ferrous chloride solution at room temperature. This was followed by elevating the pH to 10 *via* the dropwise addition of an ammonium hydroxide solution. The resulting solution was stirred

<sup>a</sup>Vanderbilt University, Institute of Imaging Science, 1161 21<sup>st</sup> Avenue South, AA 1105 MCN, Nashville, TN, 37232-2310, USA. E-mail: wellington.pham@vanderbilt.edu; Fax: +1 615 322-0734; Tel: +1 615 936-7621

<sup>b</sup>Department of Biomedical Engineering, VU Station B 351631, 5824 Stevenson Center, Nashville, TN, 37235, USA

for several hours. The synthesized particles were separated from the starting materials using deionized water, and then dialyzed into buffer representing the normal physiological concentrations of sodium citrate and sodium chloride. The concentration of iron in the solution was determined by inductively coupled plasma mass spectrometry (ICP-MS). To obtain the desired concentration of SPIO nanoparticles for analysis, a stock solution of SPIO particles was diluted 1 : 10 000 in 1% nitric acid solution. Each experiment was performed in duplicate.

## Syntheses of an epoxide linker

### Pent-4-en-1-amine

Under an atmosphere of argon, potassium phthalimide (17.21 g, 92.9 mmol) was combined with anhydrous DMF (180 mL). Afterwards, 5-bromopent-1-ene (10.0 mL, 84.4 mmol) was added slowly, and the resulting mixture was heated to 60 °C for 16 hours. The reaction was then cooled to room temperature and added to a solution of 90% NaCl water (400 mL). The resulting solution was extracted with diethyl ether (3 × 200 mL). The combined organic extracts were washed with brine (1 × 200 mL), dried over magnesium sulfate, filtered and concentrated *via* rotary evaporation to give a light yellow oil. Prolonged high vacuum pumping yielded a semi-solid (18.17 g, quant.), which was combined with ethanol (200 proof, 125 mL) in a 250 mL round-bottom flask equipped with a reflux condenser. To the heavily stirring solution, hydrazine hydrate (64% solution in water, 6.4 mL, 84.4 mmol) was added slowly. The mixture was then heated to 60 °C for 16 hours, during which time the reaction mixture formed a large amount of white precipitant. Concentrated hydrochloric acid (30 mL) was added slowly after cooling the reaction to room temperature. The reaction was heated to reflux for 3 hours and then cooled to room temperature, after which the solids were filtered out and washed with ethanol (200 proof, 100 mL) and dichloromethane (50 mL). The solvent was removed by rotary evaporation to reveal a white solid. This solid was then taken up in water (80 mL) and made basic, to litmus, by the addition of potassium hydroxide pellets. The resulting solution was extracted with diethyl ether (4 × 50 mL). The combined extracts were concentrated on a rotary evaporator at a temperature of 0 °C to reveal a light yellow oil, which was purified by short-path distillation. The product distilled over at 95–100 °C (1.463 g, 20%). <sup>1</sup>H NMR (300 MHz, CDCl<sub>3</sub>): δ 5.84–5.71 (m, 1H), 5.02–4.89 (m, 2H), 4.75 (s, 2H), 2.66 (t, *J* = 7.2 Hz, 2H), 2.06 (q, *J* = 7.1 Hz, 2H), 1.50 (p, *J* = 7.4 Hz, 2H). HRMS-ESI *m/z*: 86.0962 (C<sub>5</sub>H<sub>11</sub>N + H requires 86.0964).

### Pent-4-en-1-aminium 4-methylbenzenesulfonate

To a solution of pent-4-en-1-amine (1.463 g, 17.2 mmol) in dry diethyl ether (10.0 mL) at 0 °C was slowly added a solution of *p*-toluenesulfonic acid (3.277 g, 17.2 mmol) in dry diethyl ether (12.0 mL). This produced a white precipitant, which was filtered out and rinsed with additional cold diethyl ether (10 mL). Drying under high vacuum yielded the title compound as a white solid (2.8894 g, 65%). <sup>1</sup>H NMR (300 MHz, D<sub>2</sub>O): δ 7.64 (AA'XX', *J* = 8.2 Hz, 2H), 7.28 (AA'XX', *J* = 8.1 Hz, 2H), 5.84–5.71 (m, 1H), 5.07–4.98 (m, 2H), 2.90 (t, *J* = 7.6 Hz, 2H), 2.31 (s, 3H), 2.05 (q, *J* = 7.1 Hz, 2H), 1.66 (p, *J* = 7.5 Hz, 2H); <sup>13</sup>C NMR (75 MHz, D<sub>2</sub>O) δ 142.3, 139.4, 137.2, 129.3, 125.2, 115.6, 38.9, 29.6, 25.7, 20.4. HRMS-ESI *m/z*: 258.1164 (C<sub>12</sub>H<sub>20</sub>NO<sub>3</sub>S requires 258.1164).

### 3-(Oxiran-2-yl)propan-1-aminium 4-methylbenzenesulfonate

A fresh solution of dimethyldioxirane was prepared as follows: acetone (13.0 mL, 177 mmol), sodium bicarbonate (12.0 g, 143 mmol), and water (20 mL) were added to a 100 mL three-neck round bottom flask, which was fitted with a solid addition funnel, argon inlet and Vigreux column. Attached to the Vigreux column was a 50 mL two-neck round bottom flask equipped with a dry-ice condenser, which as then attached to a house vacuum line equipped with an inline vacuum trap. The entire setup was purged of air using a steady stream of argon. Oxone® (25.09 g, 41 mmol) was added slowly to the reaction mixture *via* the solid addition funnel over a period of 1.5 hours while stirring constantly and ensuring a steady flow of argon. Once the Oxone® addition was complete, the entire system was put under the house vacuum for a period of 1 hour. Dimethyldioxirane in acetone (20 mL, 0.099 M) was trapped in the two-neck round bottom flask, which was subsequently sealed and stored in a freezer until needed.

To a dry 25 mL round bottom flask were added pent-4-en-1-aminium 4-methylbenzenesulfonate (0.103 g, 0.40 mmol) and dry CH<sub>2</sub>Cl<sub>2</sub> (3.0 mL), which was then cooled to 0 °C under an atmosphere of argon. The freshly prepared dimethyldioxirane solution (8.0 mL, 0.84 mmol) was added slowly, and the resultant clear reaction mixture was stirred at 0 °C for a period of 3 hours. Dry diethyl ether (10 mL) was then added, which produced a white precipitant. The precipitant was filtered out and rinsed with additional cold diethyl ether (10 mL) then dried under high vacuum to afford the final product as a white solid (0.109 mg, quant.). <sup>1</sup>H NMR (300 MHz, CDCl<sub>3</sub>): δ 7.72 (AA'XX', *J* = 8.0 Hz, 2H), 7.64 (bs, 3H), 7.14 (AA'XX', *J* = 7.9 Hz, 2H), 2.83 (t, *J* = 7.5 Hz, 2H), 2.71 (m, 1H), 2.59 (t, *J* = 4.4 Hz, 1H), 2.31 (m, 4H), 1.65 (p, *J* = 7.6 Hz, 2H), 1.49 (m, 1H), 1.30 (m, 1H).

### Coupling epoxide linker with the nanoparticles

The nanoparticles were prepared as described above and resuspended in PBS at 11 mg mL<sup>-1</sup> of iron. The epoxide linker was dissolved in a stock solution at a concentration of 100 mg mL<sup>-1</sup>. By controlling the concentration of nanoparticles at 2 or 5 mg mL<sup>-1</sup>, 500× and 2000× excess epoxide linkers (the number of molecules *vs.* particles) were mixed, with the reaction performed overnight, at room temperature, with gentle stirring. The free epoxide linker was removed from the nanoparticles using Zeba Spin Columns (Thermo Scientific, Rockford, IL) following the manufacturer's recommended procedure.

### Quantification of epoxide linkers on the surface of the nanoparticles

The copy numbers of coupled epoxide linkers on the surface of each nanoparticle were determined by measuring the amine group with Fluorescamine,<sup>16</sup> and free epoxide linkers of a known amount were used as the standard. Aliquots of the control (uncoupled) and coupled nanoparticles were both pretreated with a 0.1 × 0.1 M borate buffer (pH 9.5). A Fluorescamine stock solution was prepared in acetone at 40 mg mL<sup>-1</sup>. For each tested sample and blank, Fluorescamine was added to a final concentration of 1 mg mL<sup>-1</sup>. Following the addition of Fluorescamine, the samples were mixed and allowed to stand for several minutes. Fluorescence was then determined with a 400 nm excitation and a 460 nm emission.

## Conjugation of folate and/or FITC to epoxide linker-coupled nanoparticles

NHS-folate and FITC were dissolved in dimethyl sulfoxide at a stock concentration of 12.5 or 100 mg mL<sup>-1</sup>, respectively. The pH of the epoxide linker-coupled nanoparticles was exchanged to 9.5 borate buffer using Zeba Spin Columns, and the iron concentration was adjusted to 2 mg mL<sup>-1</sup>. An aliquot of 1 mL (2mg) of nanoparticle stock solution was double-labeled with FITC and folic acid. This was accomplished by first adding 5 µL of FITC solution and stirring the mixture at room temperature for 45 minutes prior to subsequent addition of 80 µL of the NHS-folate solution. For the FITC or folic acid only labeled nanoparticles, only one reactant was added. All the reactions were performed overnight, after which the conjugated nanoparticles were separated from the unreacted folic acid and FITC by passing the reaction mixture through Zeba Spin Columns. The suspension was concentrated to 5 mg mL<sup>-1</sup> iron *via* centricon for future use.

## Quantification of the conjugated FITC and folic acid

The copy number of FITC in each nanoparticle was estimated simply by measuring the fluorescence strength of the labeled particles against the free FITC with a known concentration. The extent of folate conjugation was determined by spectrophotometric analysis at an absorbance of 358 nm ( $\epsilon = 8643.5 \text{ M}^{-1} \text{ cm}^{-1}$ ) based on a reported procedure.<sup>17</sup>

## Cell culture and uptake studies

Human kidney derived 293 (folate receptor positive) and alveolar basal epithelial derived A549 cells (lung carcinoma, folate receptor negative) were cultured in an RPMI-1640 medium supplemented with 10% fetal bovine serum, 100 U mL<sup>-1</sup> penicillin, and 100 mg mL<sup>-1</sup> streptomycin (Gibco BRL) under standard culture conditions in a humidified incubator maintained at 5% CO<sub>2</sub> at 37 °C. Cell uptake studies were performed using both cell lines with folate-conjugated or folate-free nanoparticles. A total of  $1 \times 10^6$  cells were seeded in each well of a 6-well plate. The cells were then washed with PBS, and 1.2 mL (2 mg mL<sup>-1</sup> of iron) of FITC-labeled folate-conjugated or folate-free nanoparticle suspensions in folate-free RPMI-1640 were added to each well. After 2 hours of incubation at 37 °C, the cells were washed four times with pre-cooled PBS before they were collected by scraping with a small amount of PBS. Half of the cells (0.5 million) were pelleted and examined for fluorescence by IVIS (IVIS 200, Xenogen). Images were acquired using the IVIS imaging system with excitation set at 490 nm. Fluorescence was collected through a long-pass filter and analyzed using Living Image® software version 3.0. Half of the cells were resuspended with PBS and mixed with an equal volume of 12% gelatin to produce the middle layer for a phantom comprised of 3 layers, with 12% gelatin on the top and bottom, and a 6% gelatin and cell mixture sandwiched in the middle (all gelatin solutions were prepared in PBS).

## Magnetic resonance imaging

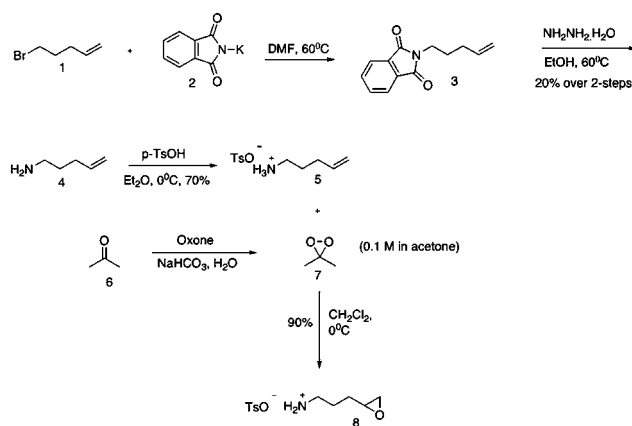
Phantom MR imaging was performed on a 4.7 T Varian Inova scanner. Suspended cells in 6% gelatin were scanned using a single slice, T2-weighted, spin-echo sequence (TR = 5 s, TE arrayed with

values of 15, 55, 95, 135, 175 and 215 ms, FOV = 40 × 40 mm<sup>2</sup>, acquisition matrix = 256 × 256 and slice thickness = 1.0 mm).

## Results and discussion

The incorporation of targeting active biomolecules onto the surface of iron nanoparticles for imaging and therapy has proven to be very useful in medical diagnostics.<sup>18</sup> Indeed, the many useful applications for functionalized iron nanoparticles, which have been conceived over the years, have made novel chemical modification of the particles even more important. The iron nanoparticles used in our study are encapsulated in dextran to enhance their size improving blood pool distribution. This coating material can render them sufficiently biocompatible and biodegradable to allow suitable *in vivo* imaging. The hydroxyl groups on the surface of the particles, as a result of this fabrication will be converted into stronger nucleophiles by employing a novel bifunctional linker. Two criteria are taken into account in designing this linker. First, it must possess a highly reactive functional group to ensure reactions with hydroxyl groups. The electrophilic group on the linker should react with the hydroxyl groups under the simplest of conditions without the use of a catalyst. Second, the other end of the linker must have a strong nucleophilic moiety to support bioconjugation studies. Epoxide reactive agents are considered ideal for this application given their stability and reactivity. Epoxides have been used widely as a suitable functionality for the development of affinity probes for protein labeling.<sup>19</sup>

As shown in Scheme 1, the synthesis of epoxy-amine linker **8** begins with the Gabriel synthesis, enabling for the conversion of 5-bromopent-1-ene **1** into the corresponding alkenylamine **4**. Protection of the newly formed amine group of compound **4** was found to be necessary prior to the formation of an epoxide, due to the fact that amines can be oxidized faster than olefins once exposed to oxidizing agents. Furthermore, the final linker product must have the amine groups blocked, since the existence of free amines would undoubtedly cause an opening of the epoxide ring *via* nucleophilic attack. Currently, the protection of amino groups in alkenylamines can be achieved using well known chemical reagents, such as Fmoc, Boc, or Cbz groups.<sup>20–22</sup> However, deprotection of these groups requires an extensive amount of work, which was not within the scope of our objectives. Instead, we used a method reported by Asensio *et al.* to protect compound **4** as an alkenylammonium



**Scheme 1** Design and syntheses of a versatile epoxy amine linker for functionalizing nanoparticles.



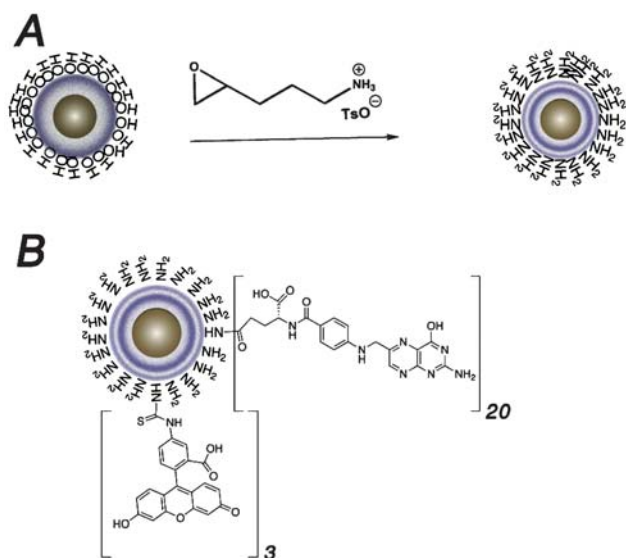


**Fig. 1** Functionalization of dextran-coated iron oxide nanoparticles with an epoxy amine linker. The process resulted in approximately 40–60 amines on the surface (A). The multivalency of aminated nanoparticles was demonstrated by incorporation of multiple numbers of different active biomaterials on the surface (B).

salt **5**.<sup>23</sup> In this approach, the protonation of amine groups is efficient enough to prevent amine oxidation by a strong electrophilic O-transfer reagent. Another unique design of this salt is that the product is compatible with the aqueous condition of nanoparticles.

Surprisingly, when using conventional reagents, such as mCPBA or hydrogen peroxide, the olefin oxidation did not progress smoothly. It is noteworthy that Asensio also made similar observation in some of the compounds. Although further investigation is needed, we cannot exclude the possible interference of the bulky counterion tosylate group. In light of this, we synthesized dioxirane **7** using a previously reported procedure.<sup>24</sup> Compound **7** converts olefin **5** into the desired epoxide linker **8** with 90% yield.

To test the feasibility of functionalizing iron nanoparticles with the newly developed linker, we treated iron nanoparticles with excess epoxide linker **8** in PBS, at physiological buffer. The conjugation was completed in an overnight reaction. To quantify the number of amines on the surface of the particles, we used the spiro dye Fluorescamine, which only reacts with free amines converting the non-fluorescent Fluorescamine to a fluorescent product, the intensity of which is proportional to the quantity of free amines. While we did observe residual fluorescence in the control group, where we incubated Fluorescamine with dextran-coated iron nanoparticles, this value was accounted for by subtraction from all the measured samples. This assay allowed us to estimate that approximately 40 to 60 copies of epoxy amine linkers were conjugated to each nanoparticle (Fig. 1A).

The abundant number of reactive amino groups on each particle renders the nanoparticles very useful for carrying a multiple copies of homogenous or heterogeneous targeting molecules for imaging or therapeutic applications. To address that notion, we labeled the aminated nanoparticles with both folic acid and FITC, sequentially. The former was activated as a succinimide ester while the latter has isothiocyanate as an amine reactive group. The extent of folate and

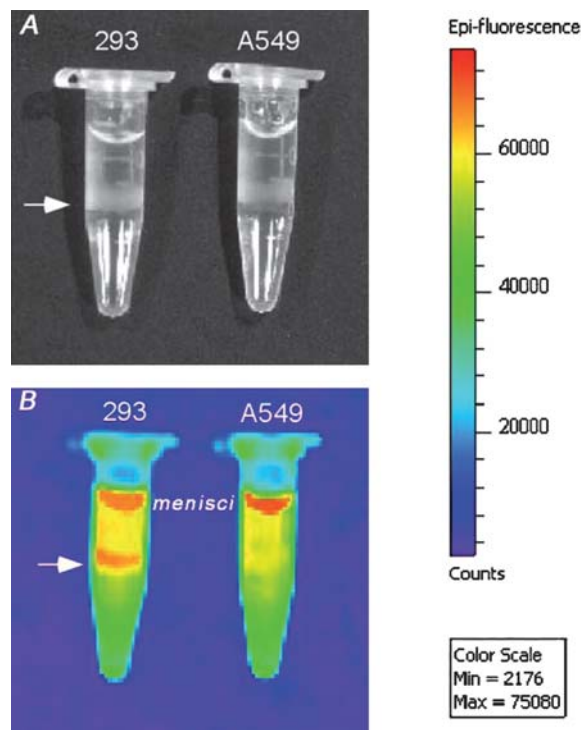


**Fig. 2** The specificity of the dual-labeled iron oxide nanoparticles in cell-based optical imaging. Folate receptor positive (293) and negative cells (A549) were incubated with the probe and imaged using white light (A) and fluorescence imaging (B).

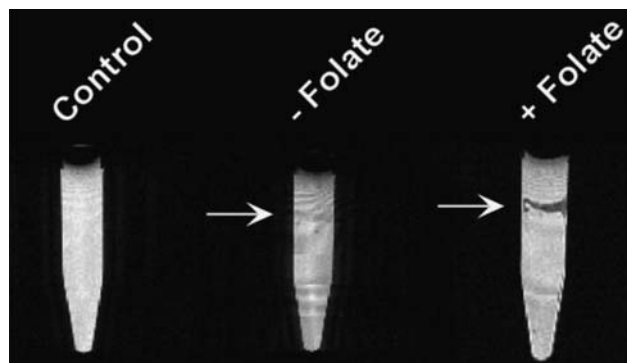


**Fig. 3** The folate receptor positive cells (293) were incubated with either aminated iron oxide nanoparticles (–Folate) or the dual-labeled probe (+Folate). The resulted cells were dispensed in gelatin-containing phantom tubes for MR imaging.

FITC conjugation of epoxy-conjugated nanoparticles was evaluated by spectrophotometric or fluorometry analysis. We found that about 20 folic acid molecules were conjugated onto the surface of one nanoparticle. While there were approximately 3 FITC molecules per nanoparticle, the dual-labeled probe remained stable for several months while stored at 4 °C (Fig. 1B).

To test the specificity of the probe, folate receptor positive (293) and negative (A549) cells were incubated with the dual-labeled probe for 2 h at 37 °C. After incubation, both cells were washed extensively with cold PBS to remove the unassociated nanoparticles. The cells were then collected and confirmed by optical or MR imaging.

As shown in Fig. 2B, the fluorescence intensity in the folate receptor (FR) positive 293 cells is stronger than that in the FR negative A549 cells. With folate-free nanoparticles, the 293 and A549 cells have similar and weak fluorescence, which suggests some nonspecific association or endocytosis (data not shown). To prove further that the fluorescence signal emanated from the folate/fluorescein conjugated nanoparticles, and not from potential residual free fluorescein or cell auto fluorescence, aliquoted cells were also assessed for iron content *via* MR imaging, as shown in Fig. 3. It was observed that the 293 cells incubated with the folate conjugated nanoparticles have greater amount of iron, evidenced by decreased signal intensity. These data suggest that the uptake of FITC-labeled nanoparticles by 293 cells occurs *via* folate receptor.

## Conclusions

In conclusion, this study was designed to provide proof of principle that the iron oxide nanoparticles could be efficiently functionalized with a linker in a mild reaction condition. We hope this study establishes a platform that impacts not only iron nanoparticles, but also other types of nanoparticles or colloids such as quantum dots, which will facilitate the effort to integrate nanotechnology with molecular imaging for biomedical applications.

## Acknowledgements

The authors thank Michio Koyama for assistance in manuscript preparation. This work is supported by a grant from NIA.

## References

- 1 J. Dobson, *Gene Ther.*, 2006, **13**, 283–287.
- 2 F. Sonvico, C. Dubernet, P. Colombo and P. Couvreur, *Curr. Pharm. Des.*, 2005, **11**, 2095–2105.
- 3 C. Xu and S. Sun, *Polym. Int.*, 2007, **56**, 821–826.
- 4 H. Gu, P. L. Ho, K. W. Tsang, L. Wang and B. Xu, *J. Am. Chem. Soc.*, 2003, **125**, 15702–15703.
- 5 Z. Teng, J. Li, F. Yan, R. Zhao and W. Yang, *J. Mater. Chem.*, 2009, **19**, 1811–1815.
- 6 Z. Medarova, W. Pham, C. Farrar, V. Petkova and A. Moore, *Nat. Med. (N. Y.)*, 2007, **13**, 372–377.
- 7 Z. Medarova, W. Pham, Y. Kim, G. Dai and A. Moore, *Int. J. Cancer*, 2006, **118**, 2796–2802.
- 8 J. Park, M. K. Yu, Y. Y. Jeong, J. W. Kim, K. Lee, V. N. Phan and S. Jon, *J. Mater. Chem.*, 2009, **19**, 6412–6417.
- 9 J. M. Perez, J. Grimm, L. Josephson and R. Weissleder, *Neoplasia (Ann Arbor, MI, U. S.)*, 2008, **10**, 1066–1072.
- 10 M. Lewin, N. Carlesso, C. H. Tung, X. W. Tang, D. Cory, D. T. Scadden and R. Weissleder, *Nat. Biotechnol.*, 2000, **18**, 410–414.
- 11 K. L. Young, C. Xu, J. Xie and S. Sun, *J. Mater. Chem.*, 2009, **19**, 6400–6406.
- 12 H. Y. Hwang, I. S. Kim, I. C. Kwon and Y. H. Kim, *J. Controlled Release*, 2008, **128**, 23–31.
- 13 J. H. Ke, J. J. Lin, J. R. Carey, J. S. Chen, C. Y. Chen and L. F. Wang, *Biomaterials*, 2010, **31**, 1707–1715.
- 14 S. Liu, B. Jia, R. Qiao, Z. Yang, Z. Yu, Z. Liu, K. Liu, J. Shi, H. Ouyang, F. Wang and M. Gao, *Mol. Pharmacol.*, 2009, **6**, 1074–1082.
- 15 S. Kobukai, R. Baheza, J. G. Cobb, J. Virostko, J. P. Xie, A. Gillman, D. Koktysh, D. Kerns, M. Does, J. C. Gore and W. Pham, *Magn. Reson. Med.*, 2010, **63**, 1383–1390.
- 16 S. Udenfriend, S. Stein, P. Bohlen, W. Dairman, W. Leimgruber and M. Weigle, *Science*, 1972, **178**, 871–872.
- 17 L. zhang, S. Hou, S. Mao, D. Wei, X. song and Y. Lu, *Int. J. Pharm.*, 2004, **287**, 155–162.
- 18 M. Gumbleton and D. J. Stephens, *Adv. Drug Delivery Rev.*, 2005, **57**, 5–15.
- 19 G. Chen, A. Heim, D. Riether, D. Yee, Y. Milgrom, M. A. Gawinowicz and D. Sames, *J. Am. Chem. Soc.*, 2003, **125**, 8130–8133.
- 20 A. Albeck and R. Persky, *J. Org. Chem.*, 1994, **59**, 653–657.
- 21 A. Jenmalm, W. Berts, Y. L. Li, K. Luthman, I. Csoregh and U. Hacksell, *J. Org. Chem.*, 1994, **59**, 1139–1148.
- 22 S. C. Wilson, P. W. Howard and D. E. Thurston, *Tetrahedron Lett.*, 1995, **36**, 6333–6336.
- 23 G. Asensio, R. Mello, C. Boix-Bernardini, M. E. Gonzalez-Nunez and G. Castellano, *J. Org. Chem.*, 1995, **60**, 3692–3699.
- 24 W. Adam, Y. Y. Chan, D. Cremer, J. Gauss, D. Scheutzwow and M. Schindler, *J. Org. Chem.*, 1987, **52**, 2800–2803.